Effect of Ti Speciation on Catalytic Performance of TS-1 in the Hydrogen Peroxide to Propylene Oxide Reaction

SUPPORTING INFORMATION FOR

The Effect of Ti Speciation on Catalytic Performance of TS-1 in the HPPO Reaction

Matteo Signorile[1], Valentina Crocellà[1], Alessandro Damin[1], Barbara Rossi[2], Carlo Lamberti[3,4], Francesca Bonino[1], and Silvia Bordiga[1]*

[1] Department of Chemistry, NIS and INSTM Reference Centre, Università di Torino, Via G. Quarello 15, I-10135 and Via P. Giuria 7, I-10125, Torino, Italy

[2] Elettra-Sincrotrone Trieste S.C.p.A. Strada Statale 14 - km 163,5 in AREA Science Park 34149 Basovizza, Trieste, Italy

[3] Department of Physics and NIS Centre, University of Turin, via Giuria 1, 10125 Torino, Italy

[4] Smart Materials Center, Southern Federal University, Zorge Street 5, 344090 Rostov-on-Don, Russia

* Corresponding author: Francesca Bonino, francesca.bonino@unito.it

Structural and morphological characterization of samples

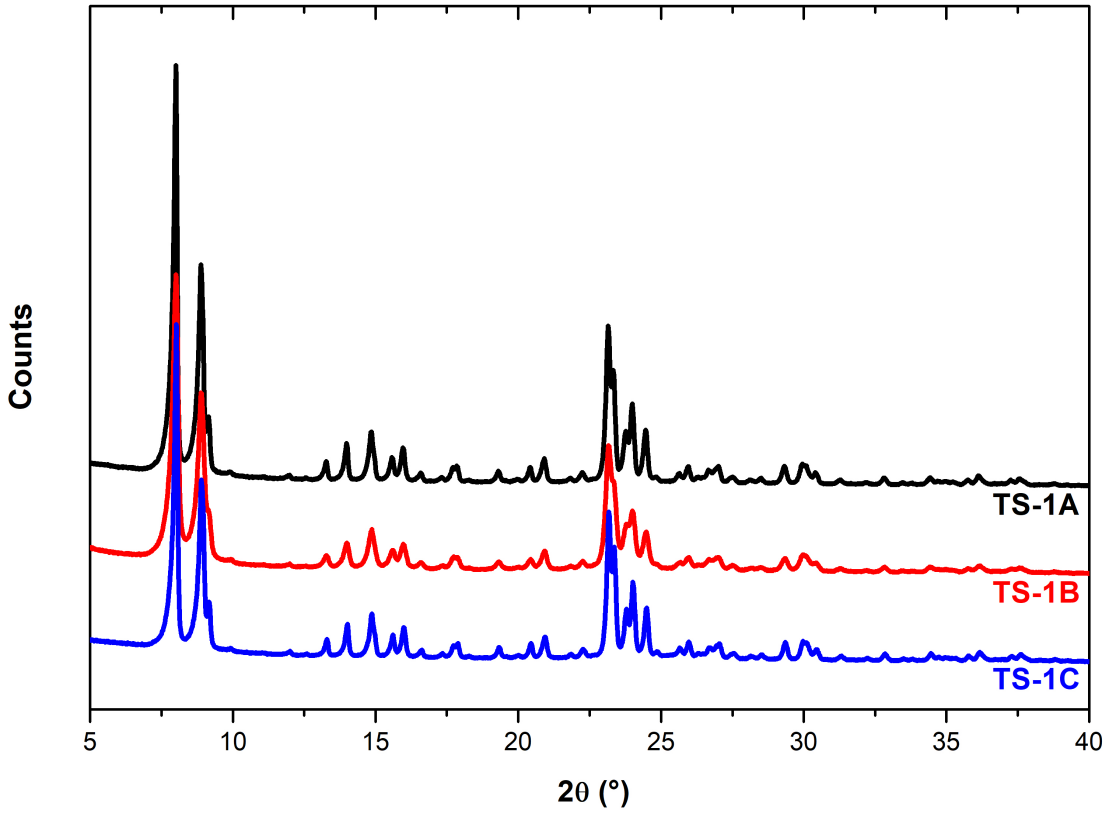

Figure S1. Powder XRD patterns of the three TS-1 catalysts.

Figure S1 shows the powder XRD patterns for the samples investigated in this work. The three catalysts are isostructural among them, with similar reflection widths suggesting they have a comparable crystal size. XRD patterns were recorded with a Panalytical X'Pert PRO diffractometer working in Bragg–Brentano geometry, using as source a Cu-anode X-rays tube (λ = 1.541 Å). A Ni filter was exploited to attenuate the k_β line. The diffracted beam was collected by a X'celerator multiple strip detector. Diffractograms were recorded in the 5–40° range, with a 200 s/° integration time and a step of 0.02°.

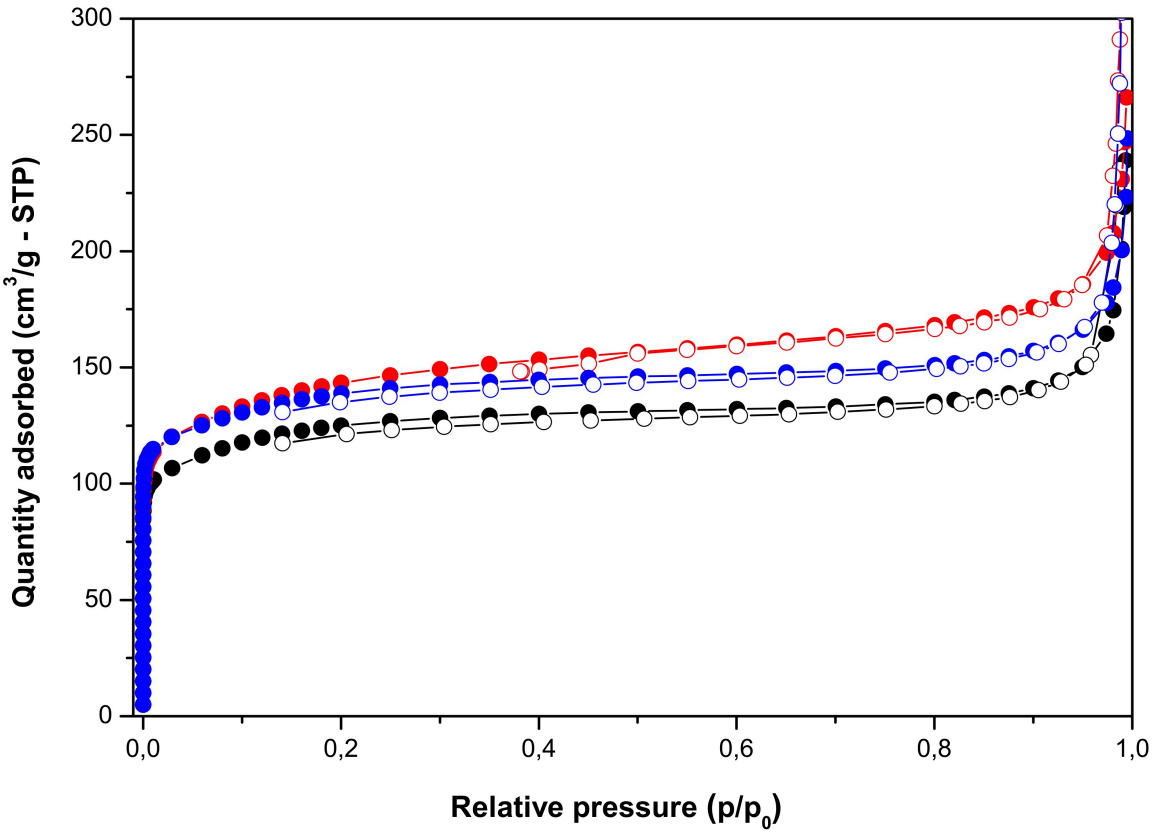

Figure S2. N_2 adsorption/desorption isotherms (performed at 77 K) of the three TS-1 catalysts.

N_2-adsorption/desorption isotherms were collected at 77 K using a Micromeritics ASAP2020 analyzer. The samples were outgassed for 4 h at 400°C before all the measurements. The specific surface areas (SSAs) were calculated by means of both the Brunauer-Emmett-Teller (BET) algorithm and the Langmuir approximation in the standard p/p_0 range. The three catalysts exhibit type I isotherms typical of microporous solids.

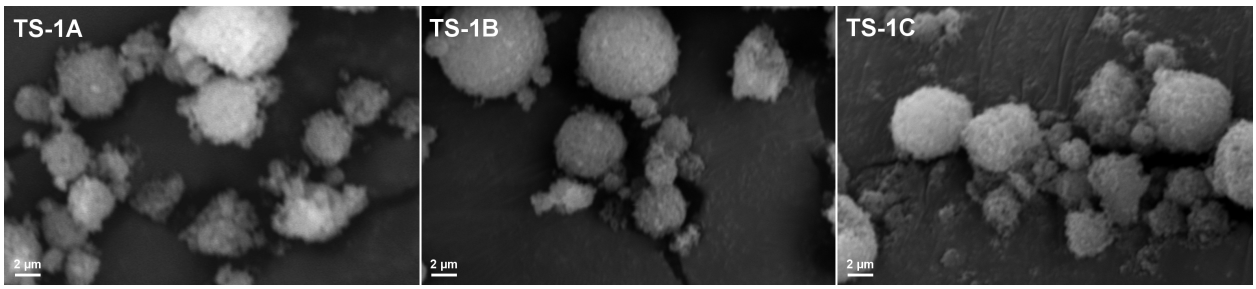

Figure S3. SEM images of the three TS-1 samples

Figure S3 shows the morphology of the three TS-1 samples considered in this work. All the materials look closely similar, being characterized by nearly spherical aggregates with heterogeneous diameters (in the 0.5-10 μm range). The transport properties of the three catalysts in the catalytic environment are thus expected to be similar, *i.e*. not being the key factor in determining the discrepancies in catalytic tests. The images were collected with a ZEISS EVO 50 XVP microscope with LaB6 source, equipped with a detector for secondary electrons. SEM measurements were performed on metal sputtered samples (gold film thickness of about 15 nm).

Effect of sample activation on Ti sites qualification

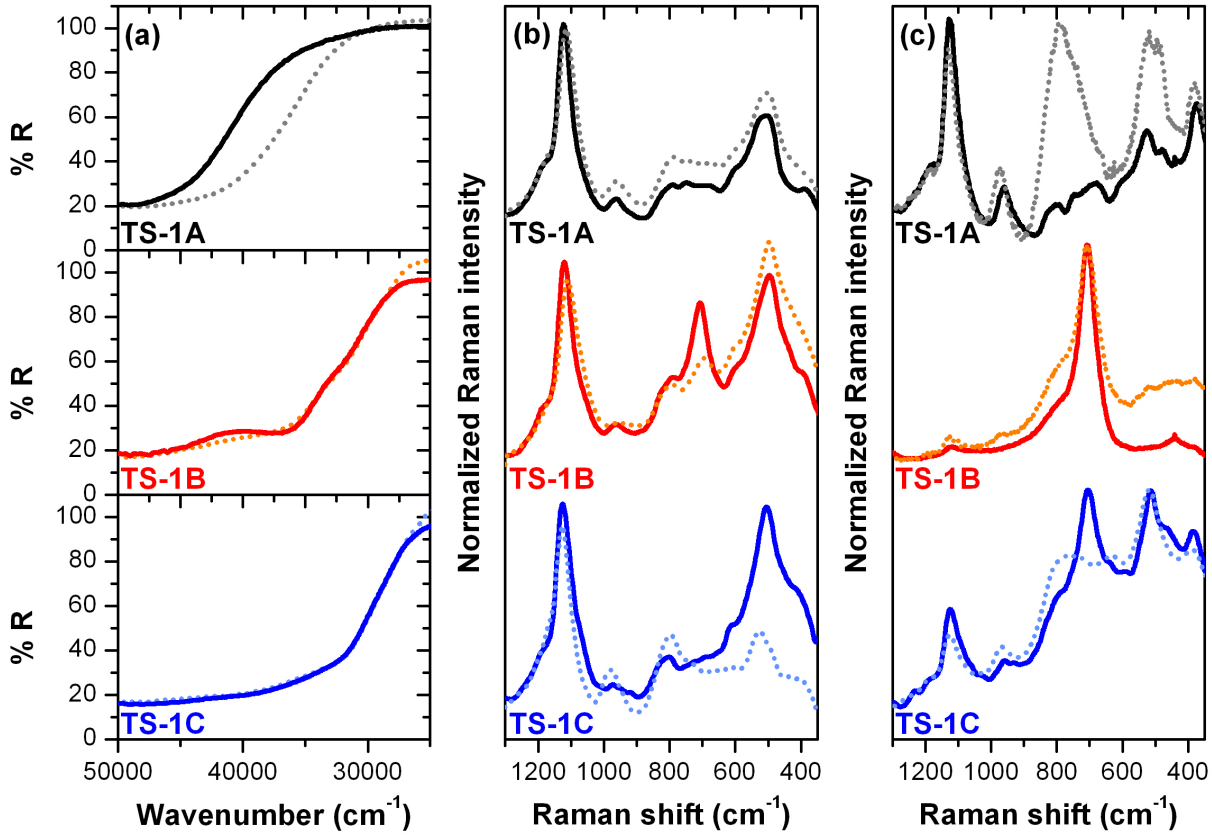

Figure S4. (a) Diffuse Reflectance UV-Vis spectra; and UV-Raman spectra collected with (b) 244 nm and c) 266 nm excitation of the three TS-1 samples, measured "as such" in air (dotted lines) and upon activation (solid lines).

In Figure S4 the effect of the sample activation on the optical and UV-Raman spectra of the TS-1 catalysts is highlighted. In the UV-Vis spectra, the most pronounced variation upon activation is observed in the case of TS-1A sample, *i.e.* containing just perfect Ti centers. The electronic transition associated to these species, located at 50000 cm^{-1}, undergoes a clear sharpening, if adsorbed molecules are removed from the microchannels of the zeolite. This is relevant in the correct evaluation of the different Ti species, as the low frequency tail, generated byperfect Ti sites in not activated materials, can hide low intensity transitions belonging to other species, *e.g.* extra-framework species. This is the case of TS-1B and TS-1C samples, where the activation

does not reduce significantly the signal width, thus revealing the presence of amorphous Ti sites and bulk TiO_2.

The UV-Raman spectra are affected by the hydration state too, as showed in panels b and c of Figure S1. The major effect concerns the TS-1A sample, containing perfect Ti sites, involving a broad and complex spectral envelope with apparent maximum at ~780 cm^{-1}. This signal has never been commented in the literature and, most probably, can be related to the vibrations of some Ti-atmospheric molecules adducts. This is particularly evident employing the 266 nm excitation: as the hydrated samples possess electronic transition in this region, probably some resonance effect is responsible for the high intensity of the 780 cm^{-1} spectral feature. Such effect can be pointed out in both samples TS-1B and TS-1C as well, in relation with their perfect sites population. For what concern the extra-framework species, as observed in TS-1B, the sample activation is really useful in facilitating their detection (*i.e.* increasing the intensity of the 700 cm^{-1} band). This effect is useful when the resonant effect of the extra-framework species is not very strong (as for example in the case of the TS-1B sample measured with the 244 nm excitation) or when the number of sites is rather low (as for example in the case of the TS-1C catalyst measured with the 266 nm excitation, thus in full resonance).

Detail of the perfect Ti signals in the 266 nm Raman spectrum of the TS-1B sample

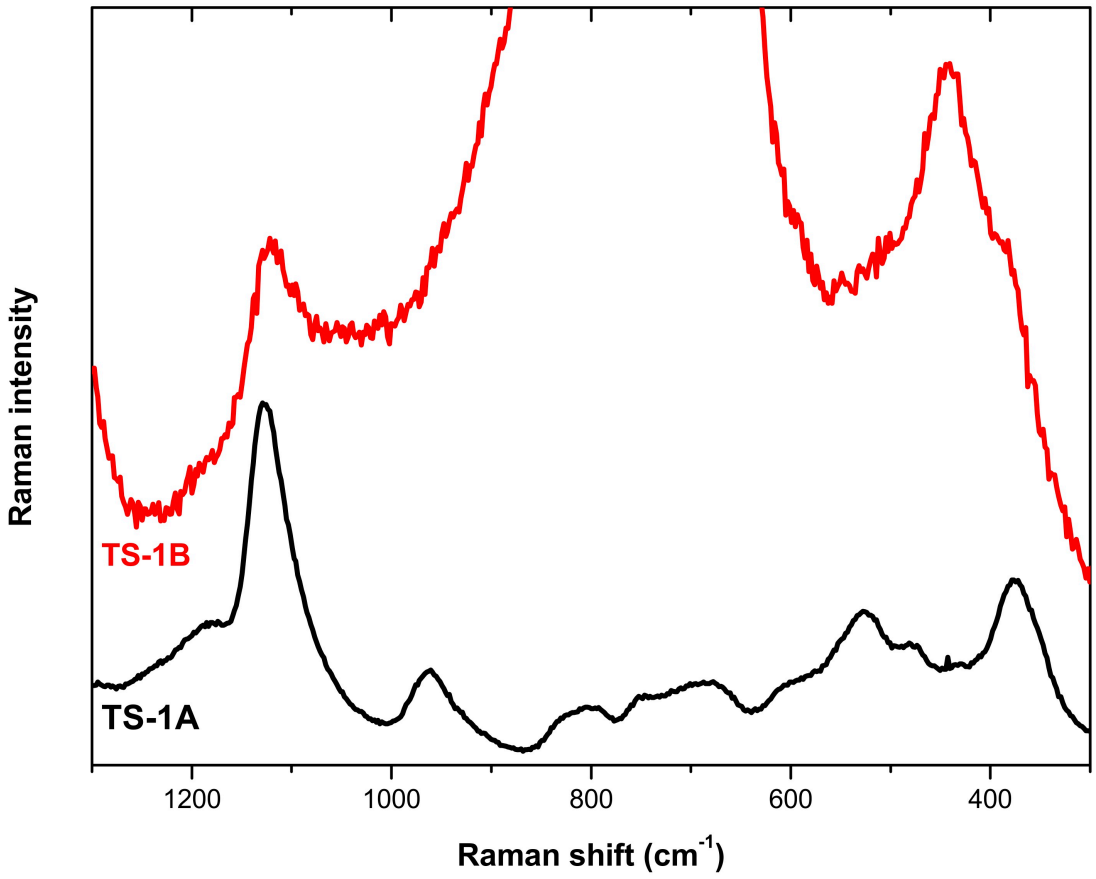

Figure S5. Comparison of the UV-Raman (266 nm excitation) spectra of the TS-1A and TS-1B samples, normalized at the 1125 cm^{-1} peak in order to improve the visualization of the features related to the perfect Ti sites.

Figure S5 shows the UV-Raman spectra (266 nm excitation) for TS-1B (and, for comparison, of TS-1A) as reported in Figure 2b, but exploiting a different normalization strategy (*i.e.* based on the 1125 cm^{-1} peak of perfect Ti sites). This strategy allows to recognize as the signals observed in the perfect sample (TS-1A) are present in TS-1B too, even if these are shadowed by the very intense peak at 700 cm^{-1}. Beside the clear 1125 cm^{-1} band, the 960 cm^{-1} and 500 cm^{-1} features are observed as weak shoulders, as well as the signal due to 5-membered rings proper of MFI topology is recognized close to 380 cm^{-1}. Interestingly, this enlarged point of view underlines the

presence of a new sharp feature centered at 445 cm^{-1}, previously unreported in the literature. Such signals could relate to the amorphous Ti species responsible for the 700 cm^{-1} peak: further characterization will be devoted to the complete understanding of this specific signal.

FT-IR spectrum of an activated TS-1 (TS-1A) in comparison with a pure defective silicalite.

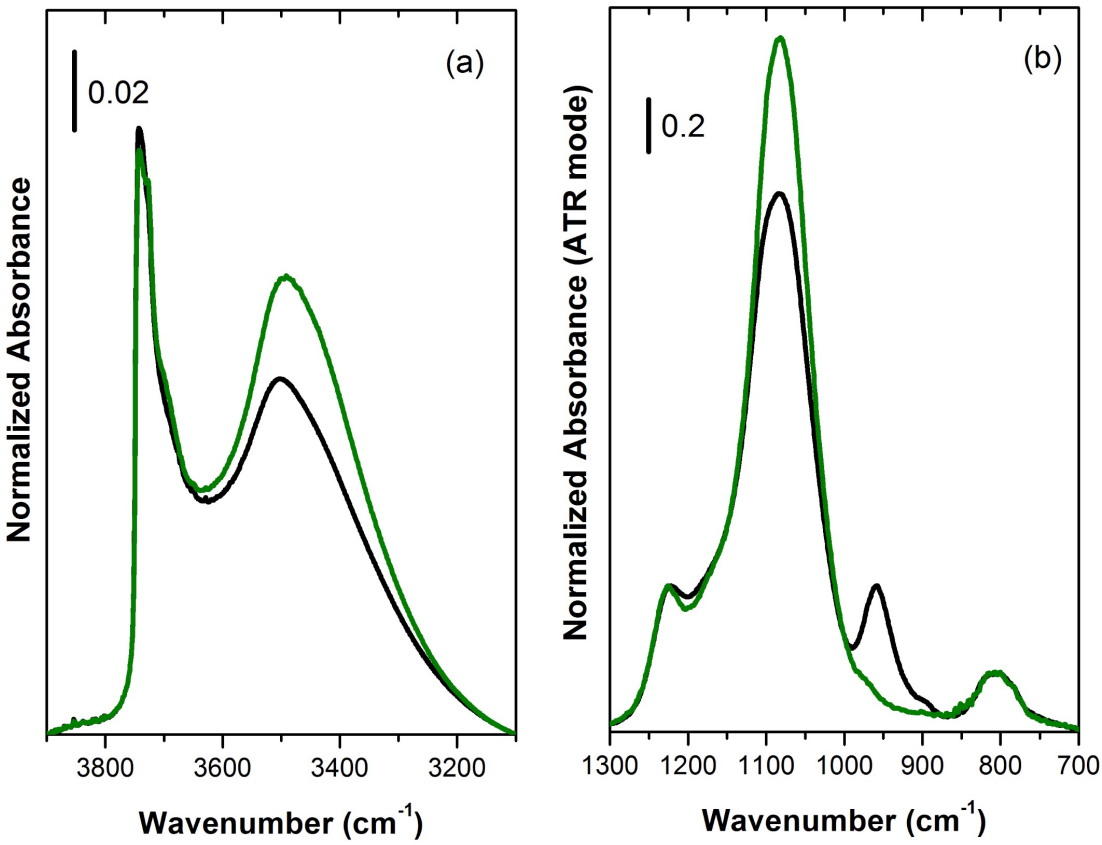

Figure S6. (a) FT-IR spectra in the OH stretching region, normalized to the TS-1 framework overtone modes, of the TS-1A sample (black) and of a pure defective silicalite (green) after activation at 500°C (b) ATR-IR spectra of the TS-1A sample (black) and of a pure defective silicalite (green) collected after activation at 500°C. The spectra have been normalized to the 800 cm^{-1} MFI framework mode.

UV-Vis check of calibration samples purity

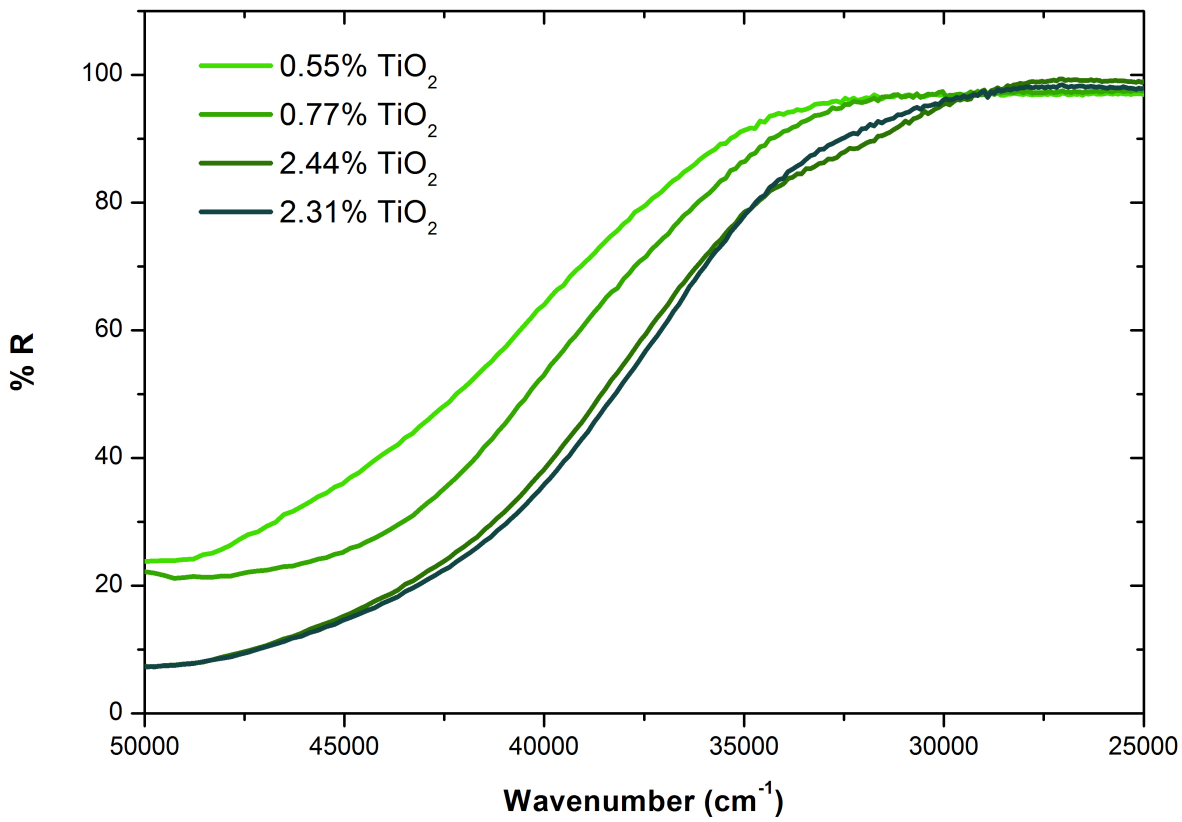

Figure S7. Diffuse Reflectance UV-Vis spectra of the perfect Ti calibration TS-1 samples, measured "as such" in air.

The purity of the four TS-1 samples exploited in the perfect Ti calibration has been verified by means of DR-UV-Vis spectroscopy (Figure S3). The absence of electronic transitions (other than the perfect Ti one at 50000 cm^{-1}) confirms the reliability of the set of samples for such procedure.

FT-IR qualitative study of external and internal hydroxyl groups: band-resolved spectra

Table S1. Integrated absorbance (Area) of the resolved spectral components I, II and III reported in Figure 5, evaluated after activation and after contact with collidine vapours.

Sample	Silanol location	Area (3745 cm^{-1}) (I, isolated)	Area (3736 cm^{-1}) (II, terminals)	Area (3724 cm^{-1}) (III, terminals)
TS-1A (activated)	Internal + external	1.24	2.67	2.05
TS-1B (activated)	Internal + external	2.43	2.85	2.40
TS-1C (activated)	Internal + external	1.21	2.63	2.50
TS-1A (collidine)	Internal	0.27	0.75	1.15
TS-1B (collidine)	Internal	0.31	1.01	1.24
TS-1C (collidine)	Internal	0.34	1.18	1.47
TS-1A (difference)	External	0.97	1.92	0.90
TS-1B (difference)	External	2.12	1.84	1.16
TS-1C (difference)	External	0.87	1.45	1.03

Extended references

(28) Dong, J.; Zhu, H.; Xiang, Y.; Wang, Y.; An, P.; Gong, Y.; Liang, Y.; Qiu, L.; Zheng, A.; Peng, X.; Lin, M.; Xu, G.; Guo, Z.; Chen, D. Toward a Unified Identification of Ti Location in the MFI Framework of High-Ti-Loaded TS-1: Combined EXAFS, XANES, and DFT Study. *J. Phys. Chem. C* **2016**, *120* (36), 20114–20124.

(42) Bordiga, S.; Roggero, I.; Ugliengo, P.; Zecchina, A.; Bolis, V.; Artioli, G.; Buzzoni, R.; Marra, G.; Rivetti, F.; Spanò, G.; Lamberti, C. Characterisation of Defective Silicalites. *J. Chem. Soc. Dalt. Trans.* **2000**, *21*, 3921–3929.

(46) D'amico, F.; Saito, M.; Bencivenga, F.; Marsi, M.; Gessini, A.; Camisasca, G.; Principi, E.; Cucini, R.; Di Fonzo, S.; Battistoni, A.; Giangrisostomi, E.; Masciovecchio, C. UV Resonant Raman Scattering Facility at Elettra. *Nucl. Instruments Methods Phys. Res. Sect. A Accel. Spectrometers, Detect. Assoc. Equip.* **2013**, *703*, 33–37.

(55) Li, C.; Xiong, G.; Xin, Q.; Liu, J. K.; Ying, P. L.; Feng, Z. C.; Li, J.; Yang, W. Bin; Wang, Y. Z.; Wang, G. R.; Liu, X. Y.; Lin, M.; Wang, X. Q.; Min, E. Z. UV Resonance Raman Spectroscopic Identification of Titanium Atoms in the Framework of TS-1 Zeolite. *Angew. Chem. Int. Ed.* **1999**, *38* (15), 2220–2222.